KU-11-5
Improving Infrastructure Sustainability II: Repairing Existing Fatigue Cracks in Steel Bridges Using CFRP Materials

By

Say Hak Bun

Eric Bonet

Adolfo Matamoros

Caroline Bennett

Jian Li

Stan Rolfe

THE UNIVERSITY OF KANSAS CENTER FOR RESEARCH, INC.

2385 Irving Hill Road – Campus West, Lawrence, Kansas 66045

Executive Summary

Distortion-induced fatigue affects a large number of bridges of the US highway system. This type of damage is commonly observed at connections between cross-frames and steel girders. The differential displacement induced by bridge traffic induces forces in the cross frames that cause out-of-plane distortion of the web, inducing highly localized stresses at the welds that tie the connection plate used to attach the cross frame to the girder.

This report describes the results of an experimental program to evaluate the use of composite materials to prevent and repair distortion-induced fatigue damage in web-gap regions of steel girders. In this method of repair, a composite block is cast in place in the area surrounding the cross-frame to girder connection to provide an alternate load path and reduce the stress demands in the welds of the connection.

Two full-depth bridge girders were subjected to dynamic loading under a constant force range and allowed to develop fatigue cracks. The girders were subsequently repaired using composite blocks and subjected to several million fatigue cycles. Test results showed that the repair method was effective in halting the propagation of fatigue cracks in the bridge girders, and that it was particularly effective when anchor bolts were attached to the girder flange.

The main body of the report focuses on the experimental study, while additional details regarding computational simulations of the composite block and fabrication techniques are provided in Appendices A and B.

Acknowledgements

Table of Contents

List of Figures

1. Introduction and Background

The presence of fatigue cracks in steel girders due to cyclic tension loading is a common problem in bridge structures around the world. Fatigue cracks that initiate at weldments or other types of geometric discontinuities propagate through structural components, potentially threatening the structural integrity of bridge structures (Adams, 2009). Repairing this type of damage is a problem that often confronts bridge maintenance engineers in the United States. In response this problem, the Minnesota Department of Transportation (Mn/DOT) sponsored a study to investigate the main causes of fatigue damage in steel bridges in the US (Lindberg and Schultz 2007). As part of their study, Lindberg and Schultz conducted a survey of bridge maintenance engineers from US state DOTs and the US Army Corps of Engineers, requesting the number and type of connection details most frequently found to exhibit fatigue damage. A total of sixteen surveys were completed resulting in a list of eleven different types of connection details, of which the most common were connections between cross frames and bridge girders. Fatigue problems in these connections originate from the practice of cutting the ends of the connection plate short of the girder flanges, leaving flexible gaps at the top and bottom of the girder web. This type of detail, commonly used prior to the mid 1980s, was adopted to avoid the presence of fatigue-sensitive weldments in regions of high tension stress, in response to transverse welds on tension flanges of European bridges in the 1930s that resulted in a number of fractures (Castiglioni et al., 1988).

Given the large number of bridges affected by distortion-induced fatigue damage at the web gaps and the importance given today to minimizing traffic disruptions during repairs, there is a need for new rehabilitation methods to extend the service life of bridge structures. Adams (2009) evaluated several different retrofit measures using Finite Element Analyses (FEA), some previously developed and others newly proposed, and concluded that fully bonded FRP blocks were one of the most effective techniques to reduce the stress demand at the web gap region of steel girders.

The primary objective of the research presented in this paper is to verify experimentally the finding by Adams (2009) that FRP blocks are an effective method to repair distortion-induced fatigue damage and extend the fatigue life of steel bridge structures. This study included six test

Trials using two different steel girder subassemblies repaired with FRP blocks to prevent further distortion-induced fatigue damage due to cyclic loading imposed by a cross frame.

2. Specimen Dimensions and Material Properties

The girder subassemblies used in the experimental study were 2.7 m (9 ft) long and 918 mm (36 in.) tall (Fig. 1). The web had cross-section dimensions of 10 x 876 mm ($^3/_8$ x 34-½ in.). The bottom and top flanges had cross-sections of 279 x 25 mm (11 x $^5/_8$ in.) and 279 x 25 mm (11 x 1.0 in.), respectively. The web, bottom flange and top flange were fabricated from steel with a nominal yield strength of 345 MPa (50 ksi). Stiffener plates were welded to the web and flanges at each end of the girder. A connection plate was welded to the web at the mid-length location of the girder. The four stiffener plates were 876-mm (34-½-in.) tall, 127-mm (5-in.) wide, and 10-mm ($^3/_8$-in.) thick. The connection plate was 873-mm (34-$^3/_8$-in.) tall, 127-mm (5-in.) wide and 10-mm ($^3/_8$-in.) thick. All stiffener and connection plates had a cropped end of 32 mm (1-¼ in.), and the weld thickness was 10 mm ($^3/_8$ in.). The girder subassemblies were attached to the reaction floor through a series of C5x9 channels. A cross-frame was used to connect the connection plate and a WT segment (Fig. 2). The cross-frame was made up of three L76 x 76 x 10-mm (L3 x 3 x $^3/_8$-in.) sections, with two of the angles in an X-configuration and the other placed horizontally. A cyclic tensile load was applied on the WT by an actuator (Figs. 1 and 2).
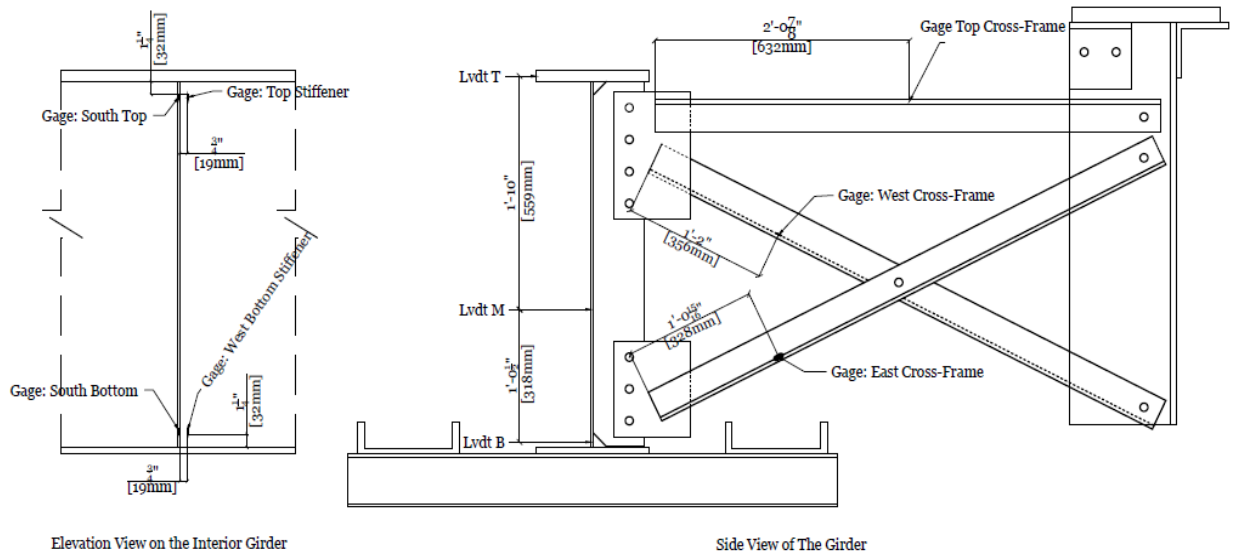
Figure 1 Girder subassembly and instrumentation.

The FRP blocks used in this study were made using randomly oriented fibers within an epoxy resin used as a binding agent. The type of resin chosen for this study was a West System™ two-part epoxy. This type of resin, commonly used for fabricating and repairing boats, was selected because it is widely available and relatively inexpensive, and resistant to fatigue damage. Two different FRP blocks were fabricated and attached to girder subassemblies with pre-formed fatigue cracks in the web gap region. The first block had mat-type glass fibers (GFRP), which was made cohesive by a styrene binder used in conjunction with the resin, while the second block was fabricated using CTS 6.4-mm (0.25-in.) chopped graphite fibers (CFRP).

The placement of the girder was inverted with respect to that expected in a bridge (Figs. 1 and 2), with the top flange free to displace laterally and the bottom flange restrained by the reaction floor (or the concrete deck in the case of a bridge).

3. Fabrication of FRP Blocks

Prior to casting the GFRP composite blocks, the paint was removed from the areas that would be bonded to the block through sandblasting. After the paint was removed, the steel surface was cleaned using a degreaser and wooden forms were placed on each side of the connection plate

to form two rectangular molds, each with dimensions of 165 x 121 x 254 mm (6-$^1/_2$ x 4-$^3/_4$ x 10 in.). The forms were firmly held in position through the use of 19-mm (¾-in.) threaded rods (Fig. 3). The threaded rods were tightened to the snug-tight condition, the mat fiberglass was placed inside the wooden forms, and the resin was cast. The resin used in the GFRP blocks was a West System™ 105 Epoxy Resin and West System™ 206 Slow Hardener, with a pot life of 25 minutes, mixed at a ratio of 5:1. The West System™ epoxy and mat fiberglass were combined to make 0.0102 m^3 (0.36 ft^3) of composite with approximately 30% mat fiberglass and 70% West System™ epoxy resin. Finally, the GFRP blocks were cured at room temperature for 24 hours before testing. It should be noted that while the threaded rods provided mechanical anchorage between the GFRP blocks, the connection plate, and the girder web, no connection beyond that of naturally-occurring adhesion during the curing process was provided between the GFRP blocks and the bottom flange of the girder subassembly.

A second girder subassembly was retrofitted using CFRP blocks. For the second subassembly the surface was prepared by grinding the paint off the specimen in the region where the retrofit would be installed. Steel anchors were installed in the girder flange by drilling and tapping, to provide mechanical anchorage for the CFRP blocks (Fig. 4). Longer bolts were installed between the connection plate and the cross frame to improve the anchorage of the CFRP blocks to the cross frame. The resin system used in the CFRP blocks was a West System™ 105 Epoxy Resin and West System™ 209 Extra Slow Hardener mixed at a ratio of 3:1. The blocks had a 15% graphite fiber volume ratio. The blocks were fabricated according to the following sequence: first, the resin and the hardener were mixed together for 30 seconds with a drill-attached paint mixer. After mixing of the liquids, the fibers were slowly added and the composite was blended with a paint stick for a period of 5 minutes. After mixing, the composite was placed in the wooden forms with mold dimensions of 127 x 152 x 178 mm (5 x 6 x 7 in.). A 51 x 102-mm (2 x 4-in.) piece of timber was used to apply pressure on the block and compact it. Additional details regarding the fabrication technique is provided in Appendix B.

4. Research Approach

The effectiveness of the composite blocks as a retrofit measure for distortion-induced fatigue damage was studied both though computer simulations and the physical simulations described in this paper. Computer simulations evaluating the performance of the composite block are described in detail in work by Adams (2009) and Richardson (2012). The study by Adams (2009) evaluated the stress demand in the web gap region of steel girders in the uncracked configuration while the study by Richardson (2012) evaluated stress demands for various crack configurations (Fig. 5). In both studies it was assumed that perfect bond existed between the composite blocks and the steel, including the girder web and flange. Adams (2009) concluded that, if properly bonded, composite blocks could bring about reductions in stress demand of at least 80% within the web gap region, while Richardson (2012) estimated a reduction on the order of 90%.

5. Instrumentation

The girder subassemblies were instrumented with three linear variable differential transformers (LVDTs) and seven Micro-Measurements WK-06-250BG-350 strain gages (Fig.1). The LVDTs were powered using a 15V power supply and measured the out-of-plane deflection at three different locations along the height of the girder. Two strain gages were placed at the top and bottom web-gaps where cracks were expected to initiate. The data was recorded at a sampling rate of approximately 10 samples/second.

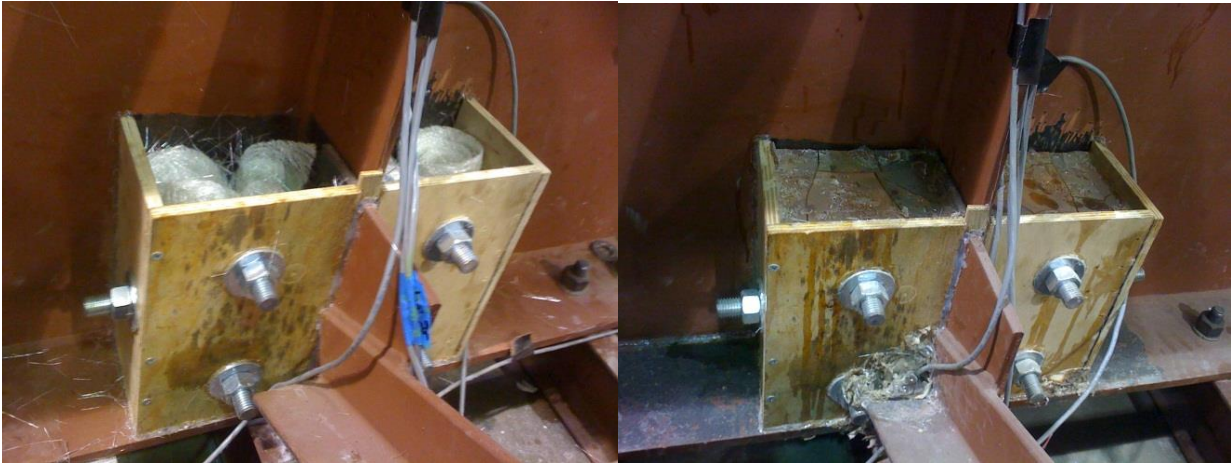**Figure 2 Girder subassembly 2 being tested at the Fatigue and Fracture Laboratory.**

Figure 3 GFRP repair block for girder subassembly 1 prior to casting the WEST resin and after curing.

6. Experimental Program

The first girder subassembly was tested under cyclic loading, ranging from 2.2 kN (0.5 kips) to 25.3 kN (5.7 kips). The test was divided into two trials: Trial G1.1 was performed on the girder subassembly without any retrofit measure, followed by Trial G1.2 in which the girder subassembly was repaired with the GFRP composite blocks. The main objective of Trial G1.1, in which the girder subassembly was subjected to cyclic loading in the unretrofitted condition, was to allow cracking to initiate and propagate. The first crack formed along the connection plate-to-web weld and was allowed to propagate to a length of 57 mm (2-¼ in.) while being inspected every thousand cycles using UV light and dye penetrant. After trial G1.1 was completed, the GFRP composite block retrofit measure was cast in the interior face of the girder, on both sides of the connection plate (Fig. 3).

Figure 4 Repair for girder subassembly 2 prior to and after casting CFRP block.
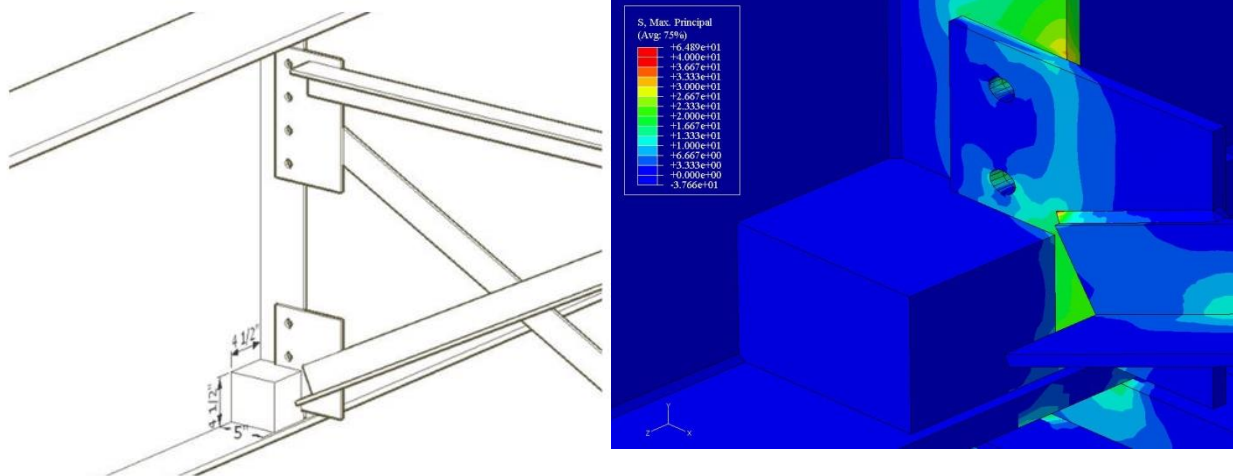
Figure 5 Configuration of FRP repair block evaluated by Richardson (2012).

After the GFRP composite blocks were installed, the girder subassembly was subjected to 1.2 million cycles (Trial G1.2). This number of cycles was chosen because in the S-N diagram of the AASHTO-LRFD Bridge Design Specifications (AASHTO 2010) it corresponds to a Category A fatigue detail at a stress range of 193 MPa (28 ksi). The 193-MPa (28-ksi) stress range was measured experimentally at the bottom web gap of an uncracked girder subassembly without any retrofit measures by Alemdar (2011), and subjected to the loading protocol used in Trials G1.1 and G1.2. Based on field measurements recently recorded at the web gap region of a bridge in Wichita Kansas with a 267-kN (60-kip) truck, it is estimated that the stress range applied to girder subassembly 1 corresponded approximately to 5 times the stress range that would be induced by the fatigue design truck load specified in the AASHTO Code. At the end of Trial G1.2, the GFRP composite blocks were removed, and the girder subassembly was then inspected for crack growth.

The loading protocol of the second girder subassembly also included multiple trials. The first trial, designated G2.1, began by applying the same cyclic tension protocol used in Trials G1.1 and G1.2 to a new uncracked and uretrofitted girder subassembly. At 35,000 loading cycles a through-thickness horseshoe-shaped fatigue crack was observed along the connection plate-to-web weld, in the web gap region. After the crack had reached a length of 38 mm (1.5 in.) Trial G2.1 was ended and the CFRP retrofit measure was applied to the bottom web gap of the girder (Fig. 3).

Trial G2.2, conducted with CFRP blocks in the bottom web gap of the girder subassembly, proceeded under the same loading protocol used in Trials G1.1, G1.2, and G2.1. The specimen was subjected to a total of 1.2 million cycles in this configuration. Because the facia side of the web gap region was unobstructed by the retrofit measure, the length of the through-thickness horseshoe-shaped crack was closely monitored throughout the entire Trial. At the end of Trial G2.2 the 38-mm (1.5-in.) horseshoe-shaped crack did not have any measurable growth, and the retrofit showed no signs of failure or debonding from the girder.

For Trial G2.3 the actuator force range was increased by 50% to a range of 3.3 kN (0.75 kips) to 36.7 kN (8.25 kips), at a rate of 2HZ. The displacement range of the actuator for this load range was approximately 12 mm (0.48 in.) compared with 8.4 mm (0.33 in.) during Trial G2.2. The specimen underwent 950,000 cycles at the increased force range (2.15 million total cycles) before an 89-mm (3.5-in.) crack was spotted along the flange-to-web weld in the top web gap region of the subassembly, which was not retrofitted. Loading continued with the same configuration and loading protocol until a total of 1.2 million cycles was reached (2.4 million total cycles in girder subassembly 2). When testing concluded the crack in the top web gap region was 165-mm (6.5-in.) long and some through-thickness cracks were observed along the connection plate in the top web gap region.

For Trial G2.4 CFRP blocks were cast in the top web gap of the girder. After the retrofit measure was successfully installed testing continued at the increased load range of 3.3 kN (0.75 kips) to 36.7 kN (8.25 kips). After 44,838 cycles a 165-mm (6.5-in.) crack was found on the gusset plate connecting the cross frame to the connection plate, in the bottom web gap region. The crack on the gusset plate was repaired multiple times until Trial G2.4 was completed with a total of the 1.2 million cycles (3.6 million total cycles). The cracks in the bottom and top web gaps showed no measurable crack growth during Trial G2.4.

7. Results

Results from the physical tests performed with girder subassembly 1 are illustrated in Figs. 6 and 7. Figure 6 presents the crack patterns recorded at the end of Trial G1.1, before applying

composite block retrofit, and at the end of Trial G1.2, after casting the GFRP blocks in the web gap region. Figure 6 shows that after the GFRP blocks were installed the observed crack growth consisted of a small spider crack on the right side of the transverse stiffener (Fig. 6). The rate of crack growth prior to and after the retrofit was applied is illustrated in Fig. 7, which shows that the crack propagation rate was reduced significantly with the retrofit measure.

One important aspect about the behavior of the GFRP block repair is that debonding between the GFRP blocks and the girder flange surfaces was observed during Trial G1.2. This behavior is inconsistent with the assumptions of the FEA simulations, in which the blocks were simulated to be perfectly bonded to the girder web and flange. The loss of bond between the GFRP blocks and the flange means that the main effect of the blocks was to decrease the stress demands at the connection plate-to-web welds by providing an alternate load path for the out-of-plane force. The force removed from the welds was distributed by the FRP block over a broader area of the web, which is consistent with the reduction in crack growth rate, and the appearance of a small spider crack on the web during Trial G1.2. A factor to be considered in the evaluation of the test results is that common bridge repair practice was not followed and that the fracture process zones at the tips of the cracks were not drilled out prior to casing the GFRP blocks. It is very likely that if the tips of the horseshoe-shaped crack had been drilled out prior to installing the GFRP blocks, no crack growth would have been observed during trial G1.2.
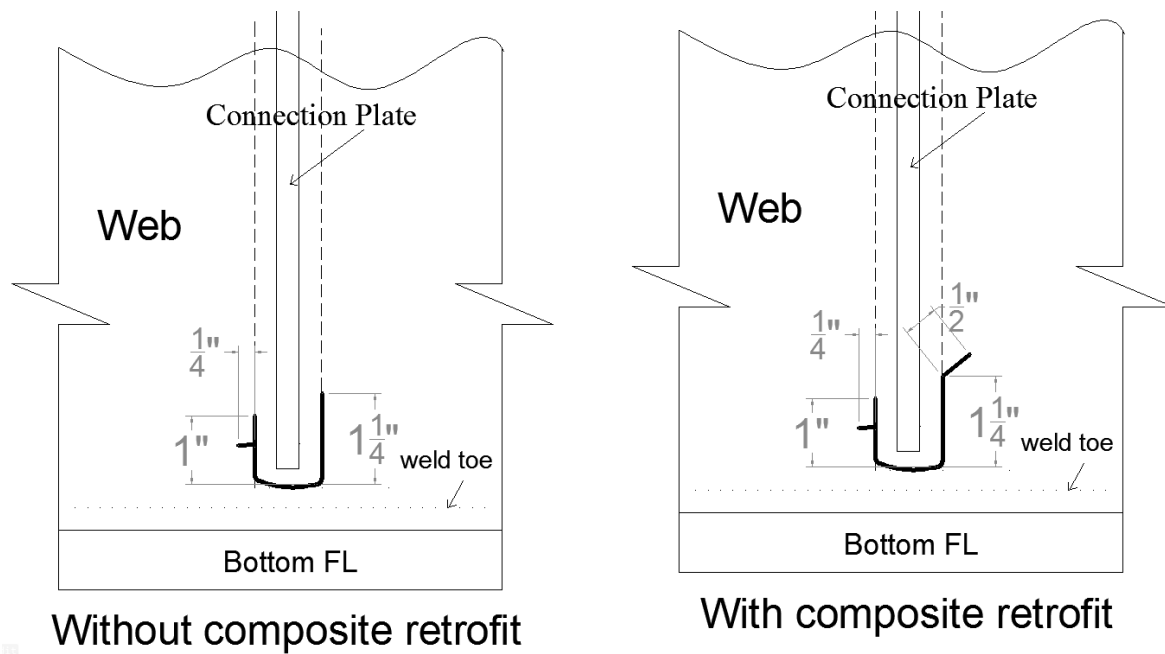
Figure 6 Observed crack patterns in girder subassembly 1 after Trial G1.1 (without composite retrofit) and after Trial G1.2 (with GFRP blocks).

As noted in the Experimental Program Section the repair with the CFRP blocks evaluated in Trials G2.2, G2.3, and G2.4 was successful in preventing any crack growth, when implemented both at the top and bottom web gaps. The CFRP repair was successful both at the load range used in Trial G1.2 to evaluate the GFRP block repair and at a load range 50% higher used in Trials G2.3 and G2.4. The main difference between the CFRP and GFRP block repairs was that mechanical anchorage was provided between the cross frame and the girder flange, instead of the cross frame and the girder web for the GFRP blocks. The connectivity between the block and the flange provided in girder subassembly 2 caused the alternate load path to transfer the force directly from the cross frame to the flange, which is more effective. The only drawback of this method of repair is that it is more difficult to fabricate at web gap regions located at the top of girders, where the presence of the concrete deck makes it more difficult to attach bolts or anchors to the flange.

8. Conclusions

The research presented in this paper was carried out to evaluate the effectiveness of two different types of FRP block retrofit measures to repair distortion-induced fatigue damage in steel bridge girders. The blocks had different manufacturing processes and different placement of mechanical anchors. The first block, fabricated with glass fiber mat and anchored to the girder web and connection plate, had a relatively small increase in crack length when subjected to a very severe stress range and for 1.2 million cycles.

The second block, fabricated with graphite fibers and anchored to the girder flange and connection plate, had no measurable crack growth when subjected to a similar stress range and number of cycles as block 1. This type of repair also had negligible crack growth in the top and bottom web gaps of the specimen when subjected to a 50% higher stress range and the same number of cycles as the GFRP repair (block 1). This repair technique proved to be slightly more effective than block 1, although it may be more difficult to fabricate.
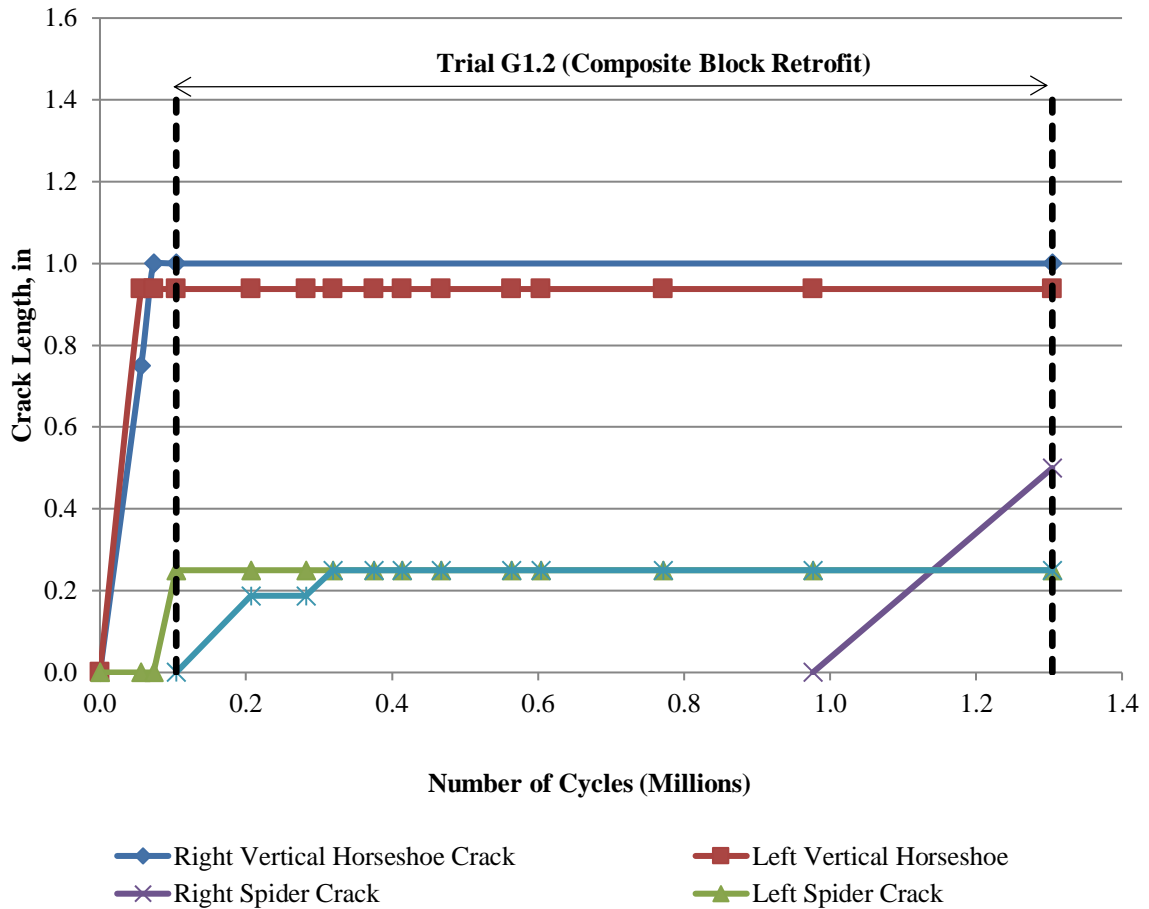
Figure 7 Crack length vs. number of cycles for girder subassembly 1

The experimental results are consistent with the findings from computer simulations performed by Richardson (2012) and Adams (2009) who showed that this type of retrofit measure could reduce the stress demand in uncracked and cracked web gap regions by 80-90%, assuming perfect bond between the composite block, the girder web, and the connection plate.

Experimental results from the six test Trials performed on the two girder subassemblies showed that the composite blocks were effective in providing an alternate load path for the out-of-plane forces imposed on the girder flange by the cross frame, significantly reducing the stress demand on the connection plate-to-girder web weldment, preventing any significant crack growth after repair. Because the study was intended to evaluate the performance of these two retrofit measures under very demanding conditions, the load range imposed on the girders was

significantly higher than that expected to occur in steel bridge structures in the state of Kansas. Furthermore, the fracture process zones near the crack tips were not removed by drilling prior to repair, and it is expected that if this common repair technique is implemented in combination with the FRP repairs the likelihood of any crack growth would be even lower.

While the retrofits studied showed significant promise in successfully repairing distortion-induced fatigue cracking, future research should be performed to optimize retrofit geometry, to examine multiple mechanical methods of ensuring bond, and to investigate long-term field durability.

9. References

AASHTO (2010). "AASHTO-LRFD Bridge Design Specifications," 5th Edition, American Association of State Highway and Transportation Officials (AASHTO), Washington D.C.

Adams, C. (2009). "Finite Element Study on Bridge Details Susceptible to Distortion-Induced Fatigue," Thesis, presented to The University of Kansas, at Lawrence, Kansas, in partial fulfillment of the requirements for the degree of Master of Science in Civil Engineering.

Alemdar, F. (2011). "Repair of bridge steel girders damaged by distortion-induced fatigue," Thesis, presented to The University of Kansas, at Lawrence, KS, in partial fulfillment of the requirements for the degree of Doctor of Philosophy in Civil Engineering.

Castiglioni, C., Fisher, J., and Yen, B. (1988). " Evaluation of Fatigue Cracking at Cross Diaphragms of a Multigirder Steel Bridge." Elsevier Ltd, 9(2):95-110.

Richardson, T. (2012). "Analytical Investigation of Repair Methods for Fatigue Cracks in Steel Bridges." Thesis, presented to The University of Kansas, at Lawrence, Kansas, in partial fulfillment of the requirements for the degree of Master of Science in Civil Engineering.

WEST SYSTEM, 105 Epoxy Resin®/206 Hardener®, 2013, http://www.westsystem.com

10. Appendix A: Computer Simulations for Development of the Second Girder Sub-Assembly Retrofit (CFRP Block

10.1. Computational Simulation Methods

The goal of the modeling effort was to develop a retrofit measure which would provide the greatest magnitude of stress reduction in the web-gap region, where fatigue cracks have already developed. The goal of the retrofit was to prevent the growth of fatigue cracks in the web-gap region. By selecting the initial retrofit through computer simulations, the most promising configuration could be tested on a physical girder.

Finite Element Models (FEMs) were created to resemble as closely as possible the girder-cross frame subassemblies that would be tested. A detailed finite element model of the 2.82-meter (9.25-ft.) subassembly was developed using ABAQUS v.6.10. The models were constructed using three-dimensional solid elements with linear-elastic material properties. Each model contained approximately 2.3 million elements and 77 million degrees of freedom. Cracks were modeled explicitly by removing a 0.8-mm (0.03-in.) strip of elements.

Steel was specified to have a modulus of elasticity of 200,000 MPa (29,000 ksi) and Poisson's ratio of 0.3. Concrete was specified to have a modulus of elasticity of 27,786 MPa (4030 ksi) and Poisson's ratio of 0.2. The modulus of elasticity of the composite was varied between 13,790 MPa (2000 ksi), 34,474 MPa (5000 ksi) and 68,948 MPa (10,000 ksi) with a Poisson's ratio of 0.2 for all three cases.

The entire steel, concrete and composite assembly was modeled in ABAQUS using primarily hexahedral (C3D8R) elements with varying mesh densities. Elements were sized as small as 0.8 mm (0.03125 in.) near regions of interest while other areas contained element sizes as large as 12.7 mm (0.5 in.). Tetrahedral (C3D4) elements were used to transition between element sizes. The concrete deck used 50.8 mm (2 in.) sized elements.

All parts, including welds, were build up separately then assembled using either surface-to-surface ties if the parts were welded together or when appropriate, hard contacts with a frictional coefficient (0.3 for steel-to-steel and composite-to-steel interactions, or 0.45 for steel-to-concrete interactions) were used to prevent parts from moving through one another during loading. The overall model geometry is presented in Figure A 1.
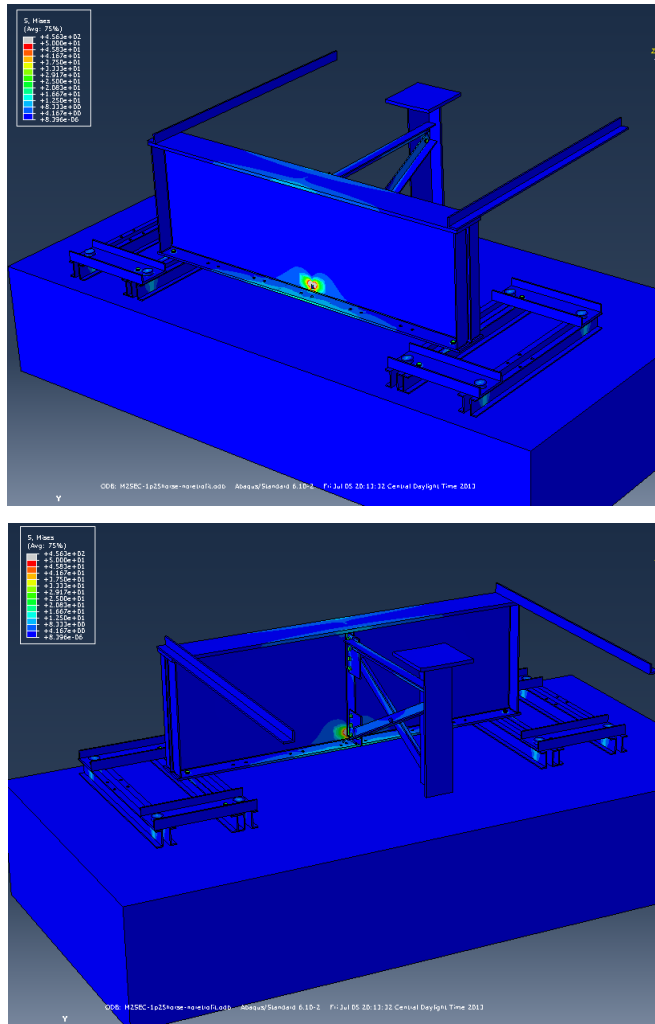
Figure A 1: View of the base finite element model: Left view of fascia side and Right view of stiffener side

Special consideration were taken to ensure the model would be constructed out of 8-node hexahedral elements only using other element types when absolutely necessary. A meshing technique was developed for bolt holes to allow for a clean mesh. Figure A 2 shows the generic bolt hole meshing technique.
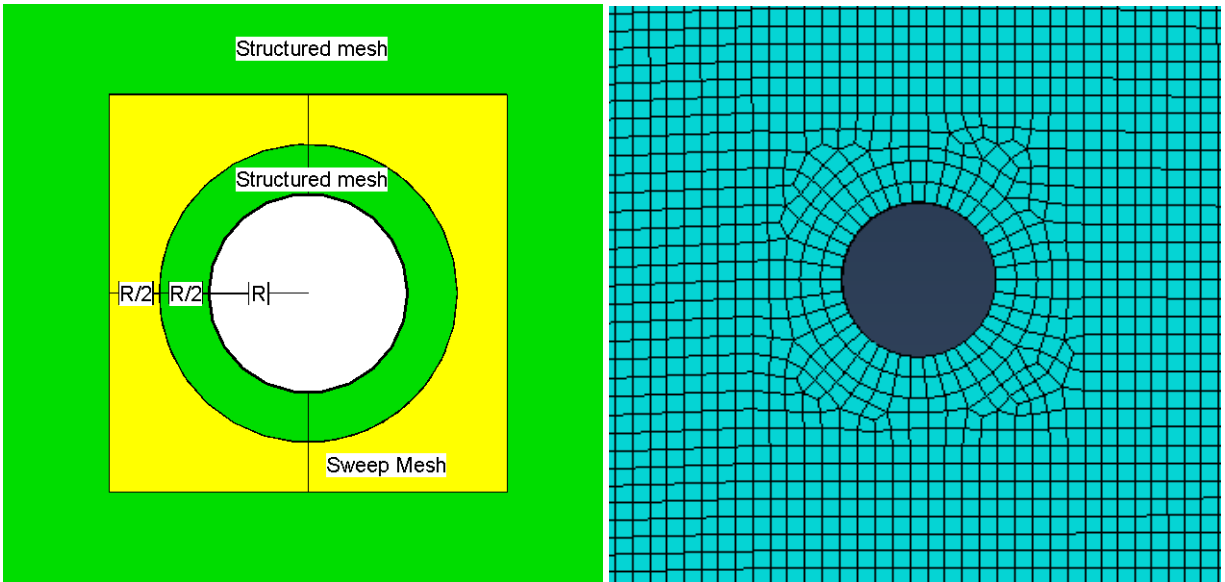
Figure A 2: Bolt hole meshing technique

Bolts were modeled as a revolution part, which was then partitioned into three parts: the shank, nut, and head. The middle of the shank was partitioned in half so the bolt load could be applied to the interior face of the shank. Figure A 3 shows the bolt meshing technique.
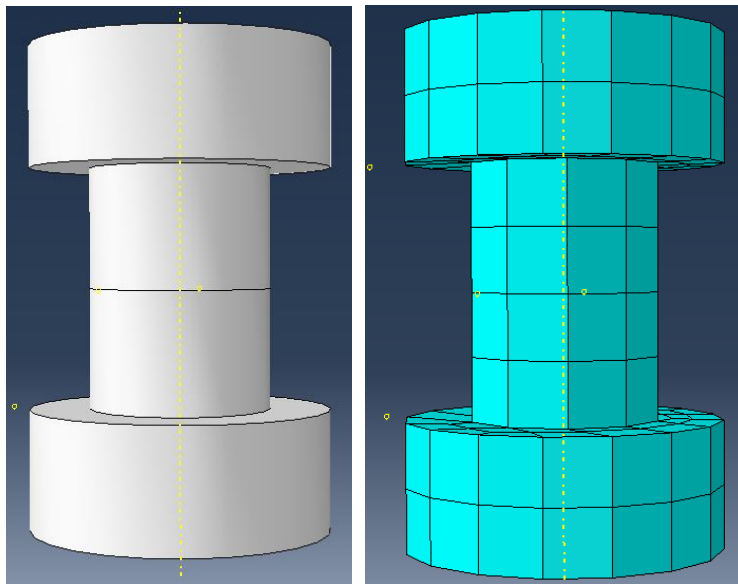

Figure A 3: Bolt meshing technique

The girder web was partitioned to allow for an extremely fine mesh to be located in the web-gap region, and have a smooth transition region to the rest of the part. 13 mm (½ in.) element sizes were used throughout the web, except in the web-gap region. In the web-gap region a 102 x 229mm (4 x 9in.) box was drawn, as shown in Figure A 4. The outer edge of the box had 13 mm (½ in.) element sizes, then another box was drawn 6.4 mm (¼ in) off of the inside faces of the 13mm (½ in.) element size box. This box used 6.4mm (¼ in) element sizes. Smaller boxes which were half the size of the next largest box were subsequently drawn off the inside faces of the larger boxes. This technique continued until the element size on the final box was 0.8mm ($\frac{1}{32}$ in). A 38mm (1 ½ in.) horseshoe crack was explicitly modeled on the web around the weld toe by removing a 0.8mm ($\frac{1}{32}$ in.) section of elements where the horseshoe crack was located.
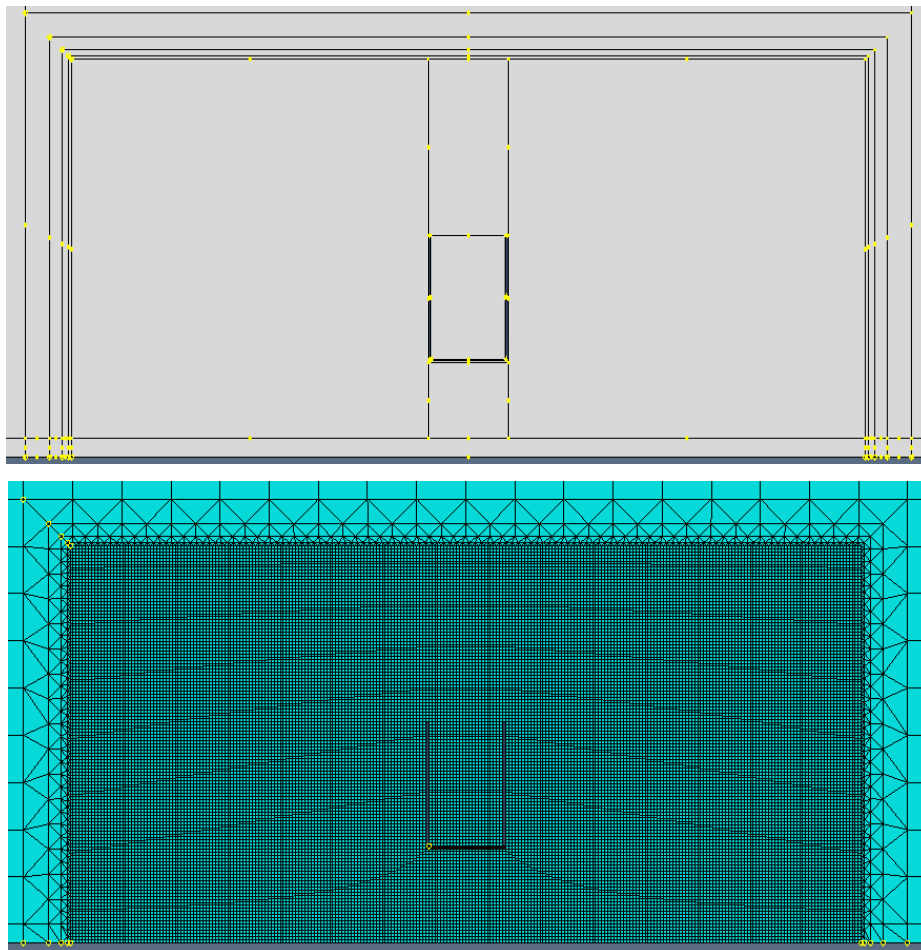

Figure A 4: Girder web meshing technique

The girder flange was partitioned using a similar step down meshing technique like the technique which was used on the web. The majority of the girder had 9.5mm ($\frac{3}{8}$ in.) element sizes except for the area located near the web-gap region where elements were 2.4mm ($\frac{3}{32}$ in.)

10.2. Retrofit Model

The stud used to connect the CFRP block to the flange was modeled the same way as bolts were modeled. The top face of the lower nut and the bottom face of the stud were tied to their respective faces of the flange. The stud was partitioned so it wouldn't be over constrained since a tie constraint was used to attach the stud to the flange and the rest of the stud had a composite-to-steel interaction with the composite block. The composite block was constructed by placing a 127x152x184mm (5x6x7in.) block on both sides of the stiffener in the web-gap region, when the studs were already in place. All parts which were located within the blocks were used to cut the blocks, removing any material from the blocks which would interfere with parts already in place. The blocks were partitioned to allow the majority of their area to have structured hexahedral elements. Swept hexahedral elements were used around hole locations and a box of tetrahedral elements were located 13mm (½ in) behind the faces of all of the holes to allow for a smooth transition back to structured hexahedral elements. shows an opaque view of the composite block, green regions represent structured hexahedral elements, yellow regions represent sweep hexahedral elements, and the four small pink regions represent the tetrahedral transition regions. Figure A 7 shows the fully meshed block using 2.4mm ($\frac{3}{32}$ in.) element sizes.
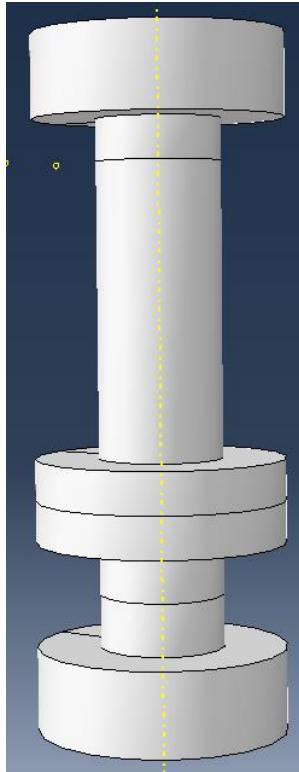
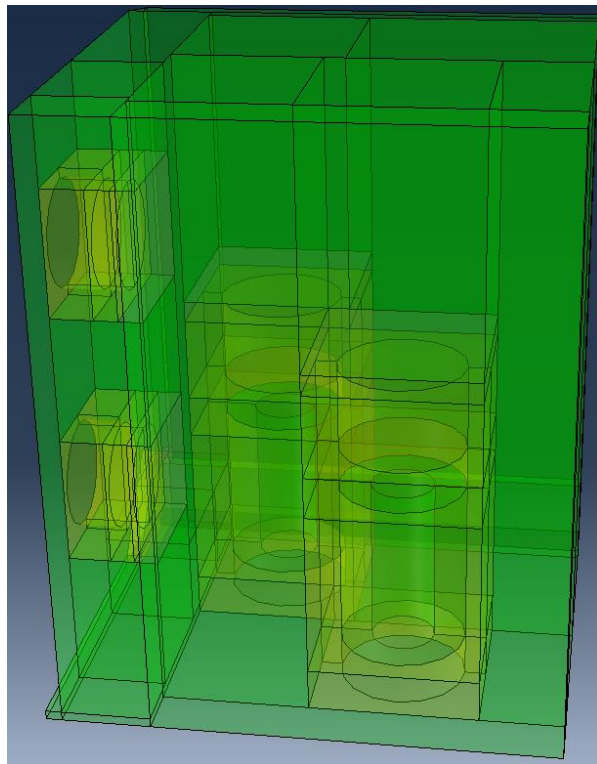**Figure A 5: Stud used to connect CFRP to the girder flange**

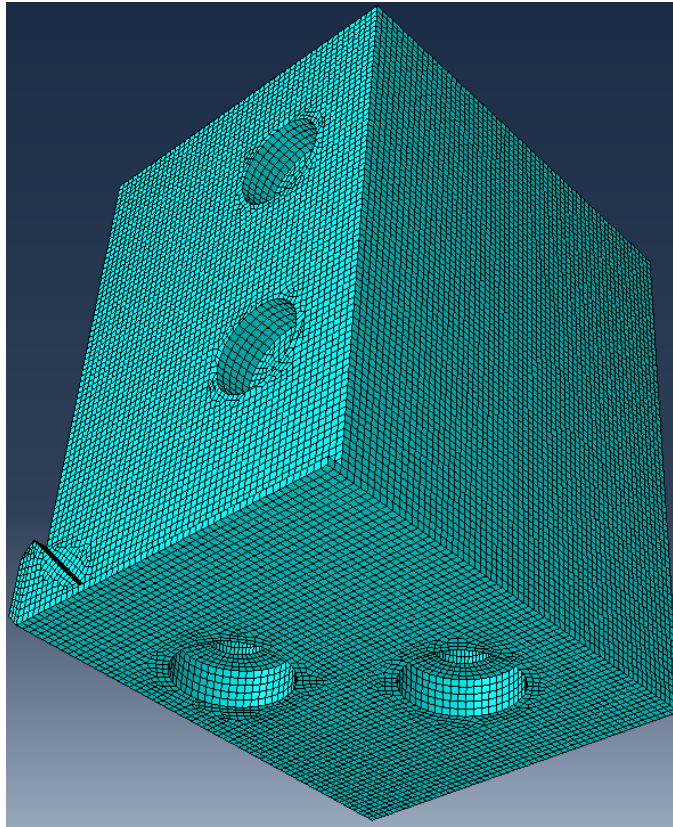**Figure A 6: Transparent view of composite block**

Figure A 7: Composite block meshing

10.3.   Loading

A bolt load of 107 kN (24kips) was applied onto each bolt as was done in experimental testing.   To improve computational efficiency, modeled bolt heads and nuts were connected directly to the surfaces they were in contact with using tie constraints. Bolt tension forces were applied in the second loading step during the computer simulations. Static actuator loading applied in the model correlated with the upper bound load of 24.5kN (5.5kip) from the initial test trial in the experimental test sequence. In the models this load was applied as an upward pressure on a (1x16x16 in) plate which was tied to the WT shape where the cross frame connected into. Actuator loading was applied during the third and final loading step during the computer simulations.

10.4.　　Results

The concept behind the retrofit that was developed was to install low modulus FRP blocks at the web-gap region, where cracking has occurred. These blocks would stiffen the web-gap region and prevent crack growth from occurring. A large fiber-volume ratio in an FRP composite block can be difficult to achieve, and the cost of fibers typically govern the cost of the FRP. A lower fiber-volume ratio typically creates a lower modulus FRP, while a large fiber-volume ratio typically creates a higher modulus FRP. For this reason low modulus FRP blocks were utilized. FEM models were constructed with a mechanical device which connected the FRP blocks to the stiffener, the web, and the flange. The analytical models with a composite block retrofit which provided positive attachment between the girder flange and connection stiffener provided the greatest stress reduction in the web-gap region. The composite blocks would prevent rotation between the connection stiffener and girder flange in the web-gap region by redistributing load to the remainder of the structure.

After numerous models were created and analyzed a mechanical connector used was developed. In the FEM models all composite-to-steel interactions were defined as a hard-contact with a coefficient of friction between the surfaces of 0.3. The stud that was embedded in an FRP block was shown to successfully reduce the stress demand, at a 38-mm (1½-in.) "horseshoe-shaped crack" around the toe of the connection stiffener to web weld, in analytical models by over 95%. The composite block retrofit geometry is shown in Figure A 8. The specific geometry of the stud was found to be effective because a large surface of it was in bearing against the girder flange preventing excessive bending from occurring. The large surface area on the top of the stud also provided a location for the composite to bear against. Figure A 9 shows the composite block retrofit used in the analytical models and Figure A 10 shows a stress path taken from the analytical models for both the retrofitted and unretrofitted specimens. The stress path is taken at a distance of half the web thickness 4.8mm (0.19 in.) away from the edge of the crack. This path was used to quantify the magnitude of stress reduction from the unretrofitted to retrofitted state.
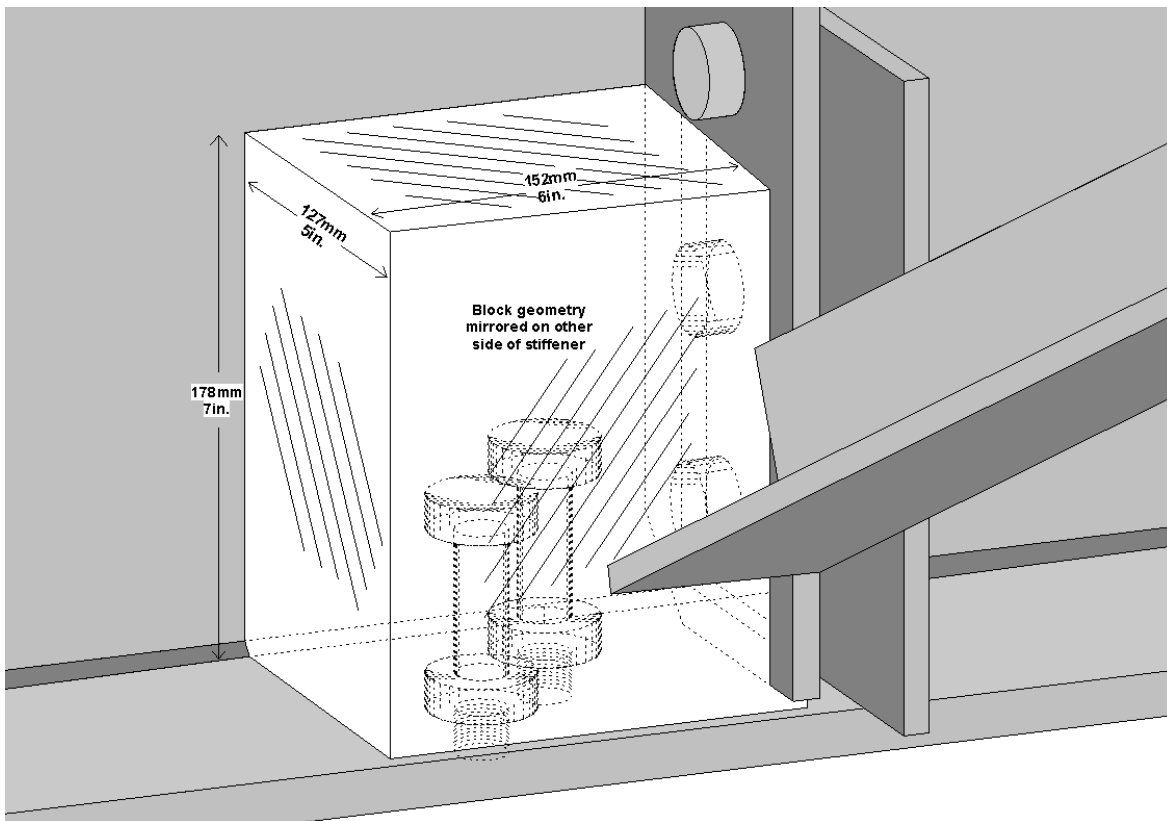
Figure A 8: Dimension of composite block retrofit

Figure A 11 presents a comparison of maximum principal stresses from the path in the unretrofitted and retrofitted models. The retrofit geometry in each retrofitted model was exactly the same, the differences in the models are the composite material properties used; the modulus of elasticity for each retrofitted model was varied. Increasing the modulus of elasticity of the composite block did not have a significant effect on the magnitude of stress reduction.

In the field the composite block retrofit would be installed by drilling and tapping holes into the top flange of the girder and subsequently installing the studs after first applying Locktite compound (or equivalent) to prevent loosening of the studs from the girder. A temporary mold would then be installed around the web-gap region. FRP would be pumped into the mold and allowed to cure. The cure time would be a function of the matrix system used and the temperature at the bridge site. After the composite has cured the mold could then be removed. Drilling and tapping the top flange of a girder, to avoid having to remove a portion of the concrete bridge deck, is not a new idea. On the Poplar Street Bridge Complex in East St. Louis, Missouri and on the Neville Island bridges which carries 1-79 near Pittsburgh, Pennsylvania, distortion-induced fatigue

28

cracks were retrofitted by attaching steel angles from the connection stiffener to the top flange of the girder (Koob et al. 1985). To accomplish this, holes were drilled and tapped into the top flange of the girder and high-strength threaded studs were installed into the holes. Steel angles were then attached to the high strength studs (Koob et al. 1985).
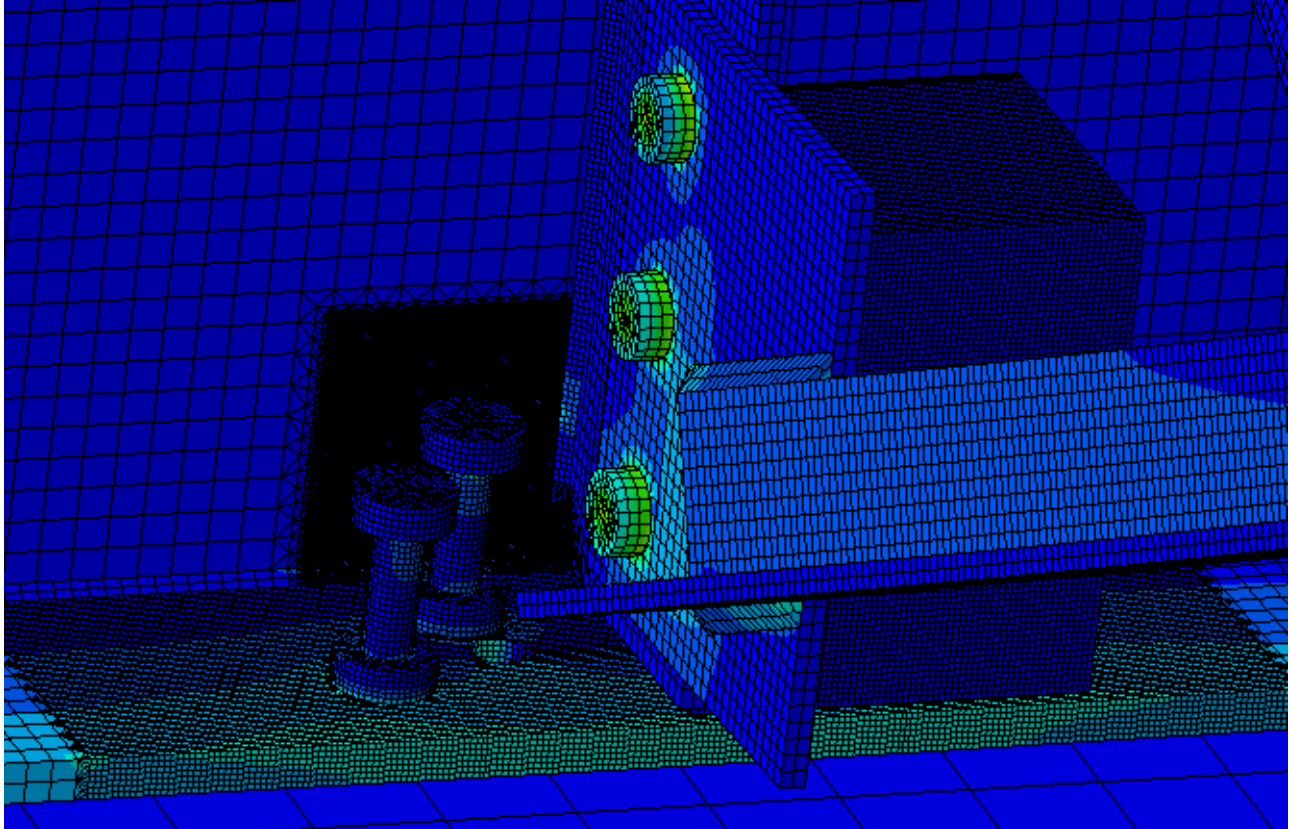

Figure A 9: Web-gap region with composite block and stud locations (left composite block was removed from view)
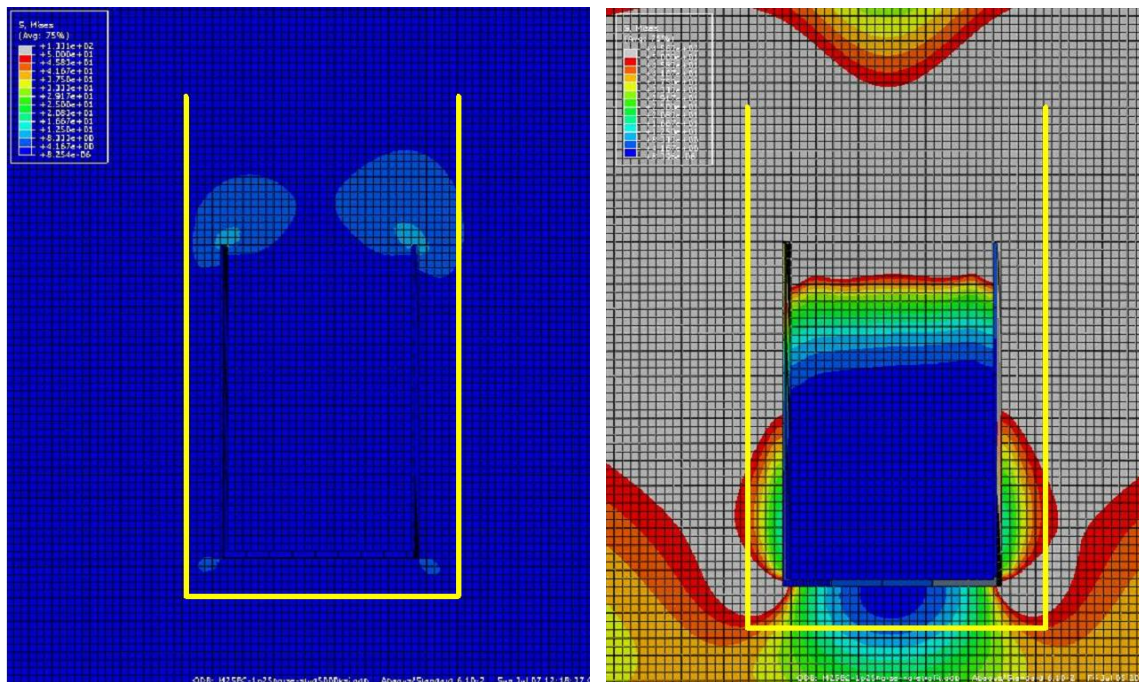
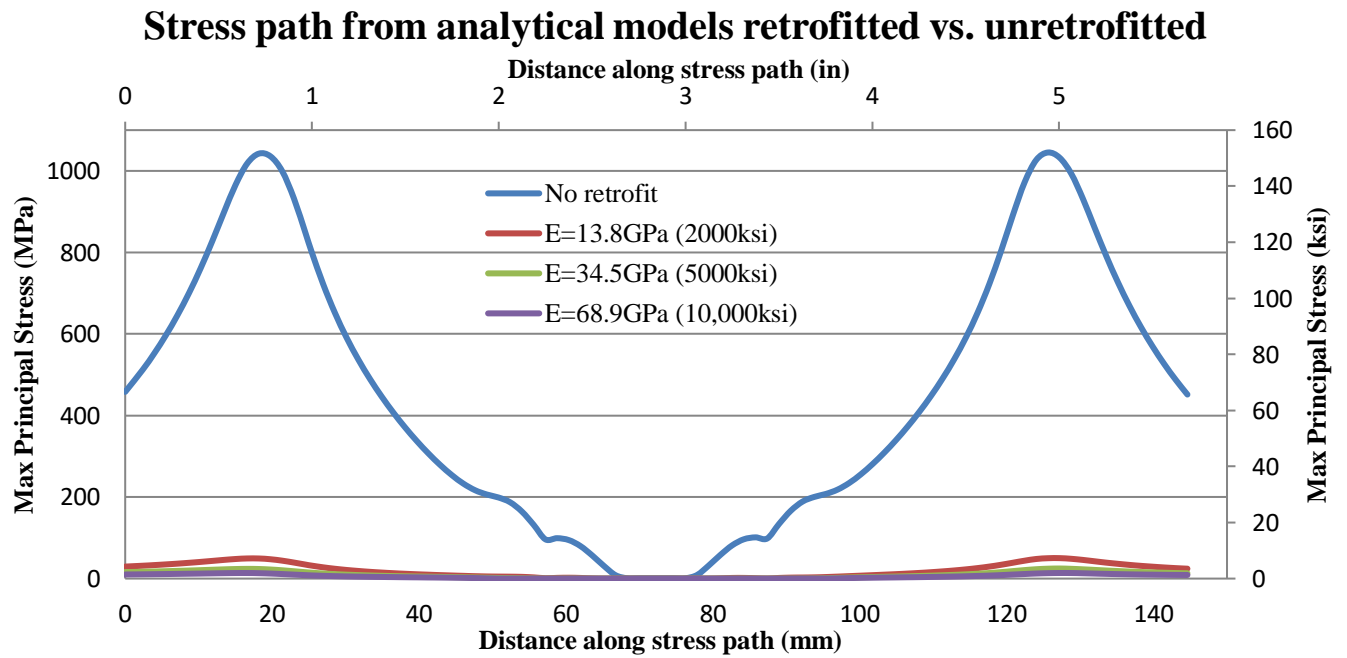**Figure A 10: HSS Path for retrofitted (left) and unretrofitted (right) FE models**

Figure A 11: Retrofitted specimen using the composite block retrofit with varying modulus of elasticity vs. unretrofitted specimen

11. Appendix B: Installation of the CFRP Block Retrofit in the Second Girder Sub-Assembly Retrofit

The materials used to apply the lower composite block retrofit were:

- West System 105 Resin

- West System 209 Hardener Extra Slow cure

- Chopped Graphite, 6.3-mm (0.25-in.) fiber length

- 38-mm (1 1/2-in.) diameter very easy to machine 1215 carbon steel rods

- 19-mm (3/4-in.) thick plywood

- 38x89-mm (2x4-in.) lumber

- Scotch Packing Tape

- DAP Dynaflex 230 Premium Indoor/Outdoor Sealant

- 19 liter (5 gallon) plastic bucket

- Drill Paint Mixer

The composite block retrofit was to be casted on either side of the connection stiffener in the web-gap region.   The first task was to fabricate the studs. The studs were fabricated out of 38-mm (1 ½-in.) diameter 1215 carbon steel rods. A metal lathe was used to machine the steel rods to their proper dimensions. The stud geometry is shown in Figure B 1.
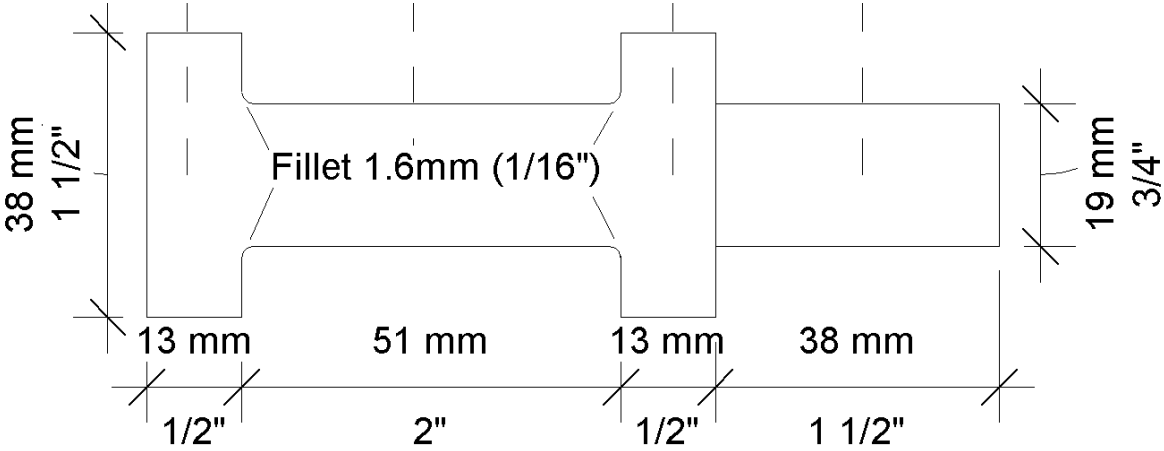

Figure B 1: Stud Geometry

In the locations where the studs were installed, holes were drilled through the bottom flange of the girder. The surface of the specimen needed to be prepared for the retrofit. This involved

using a grinder to grind all of the paint off the specimen in the region where the retrofit would be installed. Figure B 2 shows a dimensioned plan view of the hole location where the studs were installed onto the bottom flange of the girder. The two bolts closest to the bottom flange which attached the cross frame's tab plate to the connection stiffener were removed. Bolts 25-mm (1-in.) longer replaced the two bolts which were removed and a nut with the threads drilled out was placed between the head of the bolt and the connection stiffener. This nut was used to create extra surface area for the CFRP to bond to. The studs were then bolted to the bottom flange. The bolts were fully-tightened as indicated by TurnaSure Direct Tension Indicator washers. The entire region was then cleaned with Acetone. The prepared web-gap region with the studs installed is shown in Figure B 3.
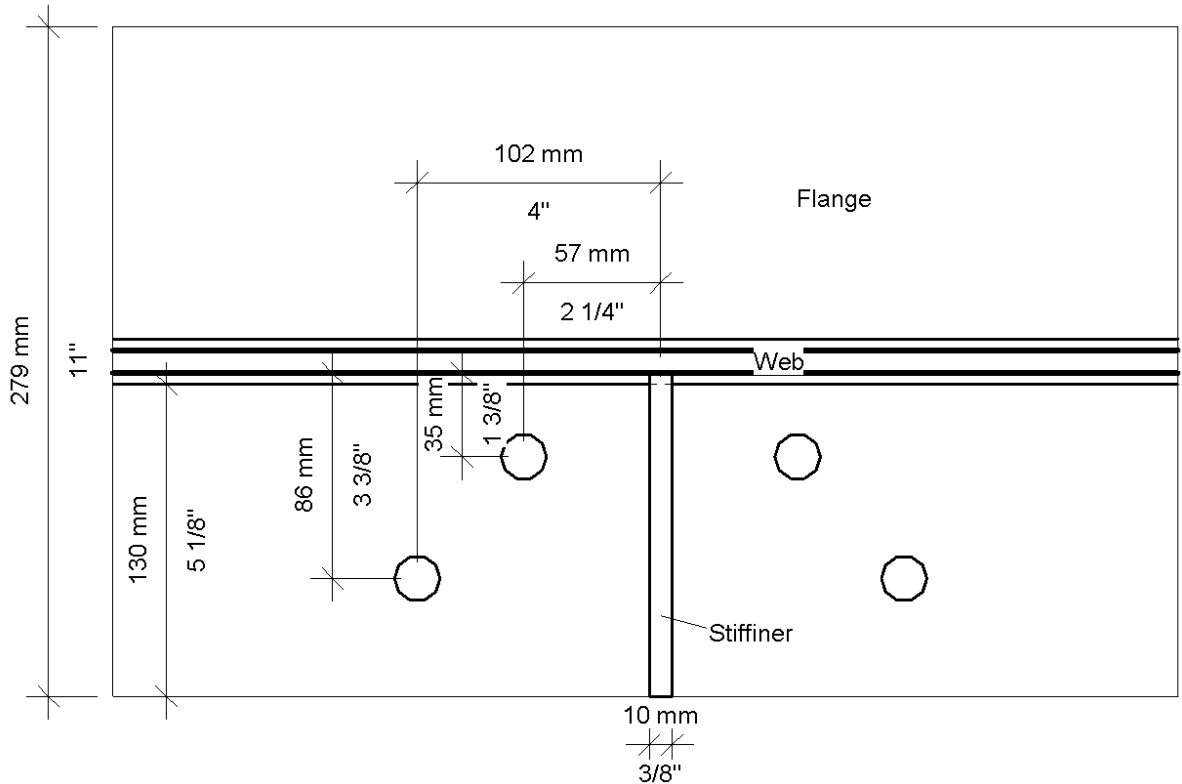

Figure B 2: Location of holes where studs were located

Figure B 3: Web-gap region prepared for the composite block retrofit

The composite block retrofit had the following dimensions 127x152x178-mm (5x6x7-in.) the block extended 127-mm (5-in.) off the web, 152-mm (6-in.) off the stiffener, and was 178-mm (7-in) tall. A mold was constructed to contain the composite during casting. The mold was constructed out of 16-mm (5/8-in) thick plywood which was cut to its proper size and then wrapped in packing tape in order to prevent the composite from bonding with the plywood. All of the edges of the mold were then caulked with Dap Dynaflex 230 Premium Indoor/Outdoor sealant in an attempt to prevent the composite from leaking during casting. The caulk was given 2 days to dry before the composite was casted. Figure 3 shows the constructed mold.

A 15% carbon fiber by volume ratio was chosen for the composite block retrofit based off the results and casting process of the composite tension test specimens. The volume of each block was 3441-cm^3 (210-in^3) giving a total volume of the two blocks of 6883-cm^3 (420-in^3). Based off the 15% fiber volume ratio 1032-cm^3 (63-in^3) of carbon fibers were required leaving 5850-cm^3 (357-in^3) of Epoxy required. As specified by West Systems the ratio of the 105 resin to 209 hardener should be 3 parts resin to 1 part hardener. Therefore, the volume of resin and hardener was 4388-cm^3 (268-in^3) and 1463-cm^3 (89-in^3) respectively. The density of the carbon fibers, West

system 105 Resin and West System 209 hardener were 27.68 g/mL, 1.142 g/mL and 0.968 g/mL respectively. All of the materials were weighed out on an Explorer Pro max 22000g scale with $1/10^{th}$ gram accuracy. The total weight of materials was, 1857.5 grams of fibers, 5011.6 grams of resin and 1415.0 grams of hardener.

After all materials were weighed out the resin and hardener was mixed together, a drill attached paint mixer was used to mix the two liquids together for 30 seconds. After the liquids were mixed the fibers were slowly added. A paint stick was used to mix the fibers and the epoxy together. After all fibers were added the composite was mixed for 5 minutes. Figure B 4 shows the composite mixture after five minutes of mixing.

Figure B 4: CFRP mixture after mixing

The CFRP mixture was then put into the mold at the web-gap region. The experimenter took handfuls of the composite and placed it into the mold until the composite was flush with the top of the box as shown in Figure B 5. A 127x152-mm (5x6-in.) piece of 16-mm (5/8-in.) thick

plywood wrapped in packing tape was placed on the top of the box. A 667-mm (26 ¼-in.) long 51x102-mm (2x4-in.) was wedged up against the underside of the girder's top flange. This 51x102-mm (2x4-in.) was used to push the plywood piece on top of the box into the form in order to compact the composite and insure there wouldn't be any air pockets present in the block. Clear epoxy then began to leak through the form insuring that the block was under pressure as shown in Figure B 6. The temperature in the lab when the block was casted was 24.3-C° (75.7-F°).

Figure B 5: CFRP inside mold

The block was given nine full days to cure. On the 10th day of curing the plywood mold was removed. A crowbar and hammer was used to remove the mold from the block. Figure B 7 shows the mold being removed and the fully cured composite block. Testing of the composite block retrofit commenced shortly after the wooden mold was removed and the lab space was cleaned.

Figure B 6: Epoxy leaking out of mold insuring air pockets wouldn't be present in the block

Figure B 7: Cured composite block